Endocrinology, en.2019-00556, https://doi.org/10.1210/en.2019-00556

Non-invasive evaluation of GPR119 agonist effects on β-cell mass in diabetic male mice using ^{111}In-exendin-4 SPECT/CT

Takaaki Murakami, Hiroyuki Fujimoto, Naotaka Fujita, Keita Hamamatsu, Koji Matsumoto, Nobuya Inagaki

Endocrinology
Endocrine Society

Submitted: July 31, 2019
Accepted: October 07, 2019
First Online: October 15, 2019

Endocrinology; Copyright 2019 DOI: 10.1210/en.2019-00556

Non-invasive evaluation of GPR119 agonist effects on β-cell mass in diabetic male mice using ^{111}In-exendin-4 SPECT/CT

Takaaki Murakami[1], Hiroyuki Fujimoto[2], Naotaka Fujita[1], Keita Hamamatsu[1], Koji Matsumoto[3], Nobuya Inagaki[1]

[1]*Department of Diabetes, Endocrinology and Nutrition, Graduate School of Medicine, Kyoto University*

[2] *Radioisotope Research Center, Agency of Health, Safety and Environment, Kyoto University*

[3] *End-Organ Disease Laboratories, Daiichi Sankyo*

ORCiD numbers:

0000-0001-8261-2593

Inagaki

Nobuya

Received 31 July 2019. Accepted 07 October 2019.

Abbreviations:

Ahx: 6-aminohexanoic acid

AUC: Area under the curve

BCM: β-cell mass

BnDTPA: Isothiocyanate-benzyl-DTPA

CT: Computed tomography

GLP-1: Glucagon-like peptide-1

GPR: G protein-coupled receptor

In: Indium

SPECT: Single-photon emission computed tomography

Longitudinal observation of pancreatic β-cell mass (BCM) remains challenging because non-invasive techniques for determining BCM *in vivo* have not been established. Such observations would be useful for the monitoring of type 2 diabetes mellitus (T2DM), a

progressive disease involving loss of pancreatic BCM and function. An ^{111}Indium (In)-labeled exendin-4 derivative ([Lys12(^{111}In-BnDTPA-Ahx)]exendin-4) targeting the glucagon-like peptide-1 receptor has been developed recently as a promising probe for quantifying BCM non-invasively. In this study, we used the ^{111}In-exendin-4 single-photon emission computed tomography/computed tomography (SPECT/CT) technique to investigate the efficacy of DS-8500a, a novel G protein-coupled receptor 119 agonist currently under investigation for T2DM treatment, in prediabetic db/db mice under dietary restriction. During the 8-week study, treatment of mice with DS-8500a delayed and attenuated the progression of glucose intolerance compared to mice under dietary restriction alone. ^{111}In-exendin-4 SPECT/CT of db/db mice revealed continuously decreasing RI intensity in the pancreas over the 8-week intervention. DS-8500a attenuated this decrease and preserved pancreatic RI accumulation compared with dietary restriction alone at the end of the observation period. This result was corroborated not only by *ex vivo* pancreatic analysis using the [Lys12(^{111}In-BnDTPA-Ahx)]exendin-4 probe but also by conventional histological BCM analysis. These results indicate that DS-8500a attenuates the progression of BCM loss beyond that of dietary restriction alone in prediabetic db/db mice. ^{111}In-exendin-4 SPECT/CT will be useful for non-invasive longitudinal investigation of BCM *in vivo*.

Introduction

Type 2 diabetes mellitus (T2DM) is a progressive disease presenting with loss of pancreatic β-cell mass (BCM) and/or function (1). Therefore, the elucidation of the effects of anti-diabetic agents on BCM is of significant value to clinical treatment strategies for diabetes.

The longitudinal changes in BCM that occur over the lifetime of a T2DM patient remain unknown because of the lack of a practical, non-invasive technique for assessing BCM *in vivo* (2). The conventional histological method of BCM analysis requires invasiveness and is limited to cross-sectional observations (2). In addition, the sampling area is restricted and may not represent the accurate changes of BCM. We have recently developed ^{111}Indium (In)-labeled exendin-4 derivative ([Lys12(^{111}In-BnDTPA-Ahx)]exendin-4) as a promising tool for β-cell imaging (3) and quantification using single-photon emission computed tomography/computed tomography (SPECT/CT) (4, 5).

The G protein-coupled receptor 119 (GPR119) is a novel receptor that recognizes oleoylethanolamide and structurally related lipids. High-level expression of GPR119 has been shown in small intestinal L cells and pancreatic β cells (6, 7). Activation of GPR119 leads to increased secretion of insulin directly from β cells and indirectly through the

stimulation of incretin secretions (6, 8). Some GPR119 agonists may stimulate β-cell replication in the pancreas of diabetic mice and islet grafts (9, 10), suggesting that GPR119 agonists may have beneficial effects on BCM. However, the development of several GPR119 agonists has been suspended because their glucose-lowering effects decreased after repeated dosing in clinical studies (11, 12).

DS-8500a is a novel oral GPR119 agonist under current investigation for T2DM treatment. DS-8500a increases glucose-stimulated insulin secretion and promotes glucagon-like peptide-1 (GLP-1) secretion in rodent models of T2DM (13, 14). In a clinical study, DS-8500a was well tolerated and significantly improved glycemic control in T2DM patients over 28 days of administration (14). Therefore, DS-8500a might be useful for investigating the effects of GPR119 stimulation on BCM in diabetic models. However, the effects of DS-8500a treatment on BCM and longitudinal BCM changes remain unclear.

This study investigates the longitudinal changes in BCM in response to treatment with the GPR119 agonist DS-8500a in diabetic mice using the ^{111}In-exendin-4 SPECT/CT technique.

Materials and Methods

Animals:

Male C57BLKS/J Iar-+Lepr^{db}/+Lepr^{db} mice (db/db) were purchased from Charles River (Tokyo, Japan). All mice were housed in a temperature-maintained environment under conditions of 14:10 light-dark cycles with free access to water and food unless otherwise stated. This animal study was approved by the animal care and use committee, Kyoto University Graduate School of Medicine (Med kyo 17534).

Diet and study design:

The mice were divided into three groups at 5 weeks old: mice fed with normal chow without dietary restriction (DR-C), mice fed with normal chow with dietary restriction (DR+C), and mice given DS-8500a under dietary restriction (DR+DS). Standard rodent chow (FR-2; Funabashi Farm, Chiba, Japan) was given as the normal chow diet. DS-8500a was administered in the form of 0.03% mixed with the normal chow diet. In mice under dietary restriction (DR+C and DR+DS groups), the daily diet was restricted to 5 g per day. The interventions started at the age of 5 weeks and implemented for 8 weeks. The weekly dietary consumption and bodyweight were recorded as well as the non-fasting blood glucose levels, determined by the glucose oxidase method (GT-1670; Arkray, Kyoto, Japan). The main comparisons in this study were conducted between the two diet-restricted groups (DR+C vs. DR+DS mice).

Mouse glycohemoglobin and GLP-1 measurements:

The glycohemoglobin levels were measured using an automated glycohemoglobin analyzer (HLC-723G8; Tosoh, Tokyo, Japan) in mice at the ages of 5 and 13 weeks. Blood samples were collected from DR+C and DR+DS mice at 13 weeks of age to measure the total plasma GLP-1 with no agent washout using the total GLP-1 ELISA kit (Meso Scale Discovery, Cat# K150JVC) (15).

Oral glucose tolerance test:

Every 4 weeks, oral glucose tolerance tests (OGTT) were performed on mice in all three groups after a 16-h fast and agent-washout period. During OGTTs, blood sample collection was performed via tail vein at 0, 15, 30, 60, and 120 min after oral glucose administration (2 g glucose/kg body weight) by oral gavage. Thereafter, the plasma glucose and insulin levels were measured using the Glucose CII Test Wako (Wako Pure Chemical Industries, Ltd., Osaka, Japan) and an insulin ELISA kit (Ultra Sensitive Mouse Insulin ELISA Kit; Morinaga Institute of Biological Science, Cat# M1104) (16), respectively.

***In vivo* ^{111}In-exendin-4 SPECT/CT:**

^{111}In-exendin-4 SPECT/CT was performed in DR+C and DR+DS mice at the ages of 5, 9, and 13 weeks. DR-C mice were also examined at 13 weeks of age. The ^{111}In-exendin-4 probe [Lys12(^{111}In-BnDTPA-Ahx)]exendin-4 was synthesized through a process involving isothiocyanate-benzyl-DTPA (BnDTPA) and 6-aminohexanoic acid (Ahx) attached to an ε-amino group at the lysine-12 residue, as previously reported (3). After an overnight agent-washout period, [Lys12(^{111}In-BnDTPA-Ahx)]exendin-4 (3.0 MBq/mouse) was injected via tail vein, and SPECT/CT imaging was performed using a Triumph LabPET12/SPECT4/CT (TriFoil Imaging Inc., Chatsworth, CA, USA), as previously reported (4). The cumulative sum of pancreatic SPECT values was analyzed using the Amira software version 5.6.0 (FEI Visualization Sciences Group, Düsseldorf, Germany). According to the previous reports (4, 5), the region of interest (ROI) was analyzed using images ranged from the lower limit of the lungs to the upper limit of the bladder, in which each voxel was 0.9 mm cube. The pancreatic ROI was determined through comparison with the outline of the kidney on a CT image, and then a 2.7 mm region surrounding the kidney was excluded in order to avoid the potential huge influence of the kidneys on the pancreas signal intensity (4, 5). The pancreatic uptake values per injected dose of the probe (%ID/g) were calculated as described in a previous report (4). Blood samples were collected just before the probe injection, and pre-SPECT total plasma GLP-1 levels were determined using the total GLP-1 ELISA kit (Meso Scale Discovery, Cat# K150JVC) (15).

***Ex vivo* pancreas analysis using the ^{111}In-exendin-4 probe:**

After the 8-week intervention, all three groups of 13-week-old mice were injected via tail vein with [Lys12(^{111}In-BnDTPA-Ahx)]exendin-4 (3.0 MBq/mouse) after an overnight agent-washout period. Mice were sacrificed by cervical dislocation 90 minutes after injection, followed by immediate resection of the pancreas and measurement of the radioactivity in the resected pancreas using a well ionization chamber, Curiemeter (IGC-7; Hitachi Aloka Medical, Ltd., Tokyo, Japan). The energy range of the Curiemeter was 30 – 3,000 keV and it could measure both peak energies of ^{111}In decay (171 and 245 keV). The half decay period of ^{111}In was set as 2.805 days. The radioactivity measurements were decay-corrected to the time of injections.

Histological analysis of BCM:

After completion of the SPECT/CT procedures, mice were sacrificed by cervical dislocation, followed by immediate resection of the pancreas. Tissues were spread on filter paper and immediately fixed in 10% formalin at 4 °C. For BCM analysis, ten sets of serial formalin-fixed paraffin-embedded sections (4 μm per section; 100 μm between each set) were stained with an anti-insulin antibody as previously reported (5). The primary antibody was a rabbit polyclonal antibody (1:100, Santa Cruz Biotechnology Cat# sc-9168) (17). The secondary antibody was Alexa Fluor 488 goat anti-rabbit antibody (1:200, Thermo Fisher Scientific Cat# A-11008) (18). The tissue sections were then stained with hematoxylin and eosin. The prepared slides were analyzed using a fluorescence microscope (BZ-X700; Keyence, Osaka, Japan). The BCM was calculated from histological sections according to the following formula: (insulin-positive area/whole pancreas area) × pancreas weight (mg), as previously reported (9).

Immunohistochemical analysis of proliferation and apoptosis:

After the 8-week intervention, formalin-fixed paraffin-embedded sections from each mouse were immunostained with guinea pig anti-insulin antibody (1:100, Abcam Cat# ab7842) (19) and rabbit anti-Ki67 antibody (1:100, Abcam Cat# ab15580) (20) as primary antibodies and Alexa Fluor 488 goat anti-guinea pig antibody (1:200, Abcam Cat# ab150185) (21) and Alexa Fluor 546 goat anti-rabbit antibody (1:200, Thermo Fisher Scientific Cat# A-11035) (22). DAPI was used for visualization of nuclei (ProLong Gold antifade reagent with DAPI; Invitrogen, Carlsbad, CA, USA). For each sample, the ratio of insulin/Ki67/DAPI co-positive cells over total insulin-positive cells was calculated. To detect apoptosis, terminal deoxynucleotidyl transferase-mediated dUTP nick end labeling (TUNEL) staining was performed using the TMR red in situ cell detection kit (Roche, Mannheim, Germany)

according to the manufacturer's instruction in parallel with the insulin and DAPI immunostaining described above. The ratio of insulin/TUNEL/DAPI co-positive cells to total insulin-positive cells was calculated for 50 islets in each mouse.

Statistical analysis:

All data are expressed as the mean ± SD. Statistical analyses were performed using one-way analysis of variance with the Tukey–Kramer post hoc test and Student's or Welch's *t*-test. We used Pearson correlation analysis to investigate correlations between two continuous variables. P-values < 0.05 were considered statistically significant.

Results

DS-8500a with dietary restriction attenuates progression of glucose intolerance in db/db mice

During the 8-week intervention, both DR+C and DR+DS mice showed a 20% decrease in dietary intake compared with the DR-C mice (Figure 1A). No significant differences in body weight were observed between the three groups at baseline (Figure 1B). Bodyweight gains of DR+C and DR+DS mice were significantly smaller than those of DR-C mice, with no significant difference between DR+C and DR+DS mice (Figure 1B). No significant differences in blood glucose levels were observed between the three groups of mice at baseline (Figure 1C). During the intervention, the non-fasting blood glucose levels of DR-C mice increased significantly more than those of the other groups (Figure 1C). DR+DS mice had significantly lower non-fasting blood glucose levels from 10 to 14 weeks of age, than did DR+C mice (Figure 1C). No significant differences in glycohemoglobin levels were observed between the three groups of mice at baseline (Figure 1D). In 13-week-old mice, the glycohemoglobin levels of DR+DS mice were significantly lower than those of DR-C and DR+C mice, with DR+C mice having significantly lower glycohemoglobin levels than DR-C mice (Figure 1D). GPR119 agonists are reported to stimulate GLP-1 secretion, but their long-term efficacy is unclear (11,12). Thus, we also examined total plasma GLP-1 levels at the end of our intervention. At 13 weeks of age, DR+DS mice showed significantly higher total plasma GLP-1 levels than DR+C mice (DR+DS vs. DR+C, 25.2 ± 8.3 vs. 10.4 ± 8.5 pg/mL; n = 5 vs. 4; P = 0.03). In addition, OGTTs after agent washout were performed on all three groups at 5, 9, and 13 weeks of age. While no significant differences in plasma glucose and insulin levels were observed between the three groups at any sampling time point at 5 weeks of age (Figure 2A), the plasma glucose levels tended to be higher in DR-C mice than in DR+C and DR+DS mice. The area under the curve (AUC)-glucose was significantly higher in DR-C mice than in DR+DS mice at 9 weeks of age (Figure 2A and 2B). The plasma

insulin levels and AUC-insulin tended to be higher in DR+DS mice than in the other groups. At 13 weeks, DR+DS mice showed significantly lower levels of plasma glucose at 15, 30, and 120 min after oral glucose administration than DR-C mice, while AUC-glucose was significantly lower in DR+DS mice than in DR-C and DR+C mice (Figure 2A and 2B). Plasma insulin levels at 30 and 60 min and AUC-insulin were significantly higher in DR+DS mice than in DR-C mice. AUC-insulin in DR+DS mice also tended to be higher than in DR+C mice (Figure 2A and 2B).

DS-8500a attenuates BCM loss in db/db mice as assessed by non-invasive longitudinal BCM analysis using ^{111}In-exendin-4 SPECT/CT

^{111}In-exendin-4 SPECT/CT was performed on mice at ages 5 (baseline), 9, and 13 weeks. Because GPR119 agonists increase plasma levels of GLP-1 (6, 8) and the possibility of interference with our probe remained, we examined pre-SPECT total plasma GLP-1 concentrations. Throughout the observation period, no significant differences in the pre-SPECT total plasma GLP-1 levels were observed between the DR+C and DR+DS mice (DR+DS vs. DR+C, 31.0 ± 8.1 vs. 35.7 ± 11.6 pg/mL at 5 weeks of age; P = 0.58, 27.8 ± 5.4 vs. 25.7 ± 14.8 pg/mL at 9 weeks of age; P = 0.83, 16.0 ± 7.7 vs. 15.7 ± 5.8 pg/mL at 13 weeks of age; P = 0.95). Representative SPECT/CT images for each group of db/db mice at 13 weeks of age are shown in Figure 3. Baseline pancreatic uptake values at 5 weeks of age did not differ significantly between the DR+C and DR+DS mice (Figure 4A). Although the pancreatic uptake values of both groups decreased at the age of 9 weeks compared to baseline, those of DR+DS mice decreased more gradually. In addition, the pancreatic uptake values were significantly higher in DR+DS than in DR+C mice (Figure 4A). Furthermore, at 13 weeks of age, the pancreatic uptake values were significantly higher in DR+DS mice than in DR-C and DR+C mice (Figure 4B). Also, the pancreatic uptake values were significantly higher in DR+C mice than in DR-C mice (Figure 4B).

***Ex vivo* pancreas analysis corroborates ^{111}In-exendin-4 SPECT/CT results indicating preservation of BCM in db/db mice treated with DS-8500a and dietary restriction**

To corroborate the BCM results of ^{111}In-exendin-4 SPECT/CT analysis, *ex vivo* pancreas analysis using [Lys12(^{111}In-BnDTPA-Ahx)]exendin-4 was performed after the 8-week intervention. RI counts of resected pancreas per injected dose of the probe were significantly higher in DR+DS mice than in DR-C and DR+C mice (Figure 4C), supporting the *in vivo* SPECT/CT results (Figure 4B).

Histological analysis corroborates ^{111}In-exendin-4 SPECT/CT results indicating preservation of BCM in db/db mice treated with DS-8500a and dietary restriction

To further corroborate the BCM results of ^{111}In-exendin-4 SPECT/CT analysis, conventional histological analysis of BCM (5) was also performed at 13 weeks of age. The results demonstrated that the BCM was significantly larger in DR+DS mice than in DR-C and DR+C mice (Figure 5A). DR+C mice tended to have a larger BCM than DR-C mice, although the difference was not statistically significant (Figure 5A). Moreover, there was a significant correlation between the pancreatic uptake values measured from the ^{111}In-exendin-4 SPECT/CT scans and histologically calculated BCM in 13-week-old db/db mice ($r = 0.93$, $P < 0.01$; Fig. 5B). In the immunohistochemical analysis of the pancreas, DR+DS mice showed significantly higher ratio of insulin/Ki67/DAPI co-positive cells to total insulin-positive cells than DR+C mice (Figure 5C). The insulin/TUNEL/DAPI co-positive ratio to total insulin-positive cells tended to be lower in DR+DS than in DR+C mice (Figure 5D).

Discussion

This study investigated the effect of GPR119 agonists on the BCM in prediabetic db/db mice. During the 8-week intervention, treatment with the GPR119 agonist DS-8500a resulted in greater preservation of pancreatic BCM as well as glucose-stimulated insulin secretions as compared to those solely under dietary restriction. BCM preservation was further confirmed by *in vivo* ^{111}In-exendin-4 SPECT/CT, *ex vivo* pancreas analysis, and conventional histological analysis. Moreover, ^{111}In-exendin-4 SPECT/CT revealed the longitudinal BCM changes non-invasively and indicated the difference in BCM loss between diet-restricted db/db mice with and without GPR119 agonist treatment.

We observed that treatment with DS-8500a in addition to dietary restriction delayed the onset of diabetes and attenuated diabetes progression in prediabetic db/db mice (Figure 1C, 1D, and 2). At the same time, BCM preservation was greatest in db/db mice treated with DS-8500a under dietary restriction, followed by those untreated but dietary restricted, and least in those without DS-8500a or dietary restriction (Figure 4 and 5A). It is well established that dietary restriction reduces glycohemoglobin levels and body weight and should be applied clinically as a first-line treatment option for T2DM. As previously shown in db/db mice (15), dietary restriction itself ameliorates β-cell loss through suppression of cellular apoptosis and oxidative stress. Our observations of the BCM in mice with and without dietary restriction (DR+C and DR-C, respectively) are compatible with these results, although the caloric reduction in the previous report was greater than ours (15). Therefore, diet restriction should have played an important role in delaying the onset of diabetes and attenuating diabetes progression in db/db mice treated both with and without DS-8500a. Moreover, it is

also noted that the ^{111}In-exendin-4 probe replicated the preservation of BCM with dietary restriction *in vivo* and *ex vivo* (Figure 4A and 4B).

GPR119 contributes to the regulation of glycemic control through increasing the secretion of GLP-1 and glucose-dependent insulinotropic peptide (GIP) in intestinal cells (6). In addition, the activation of GPR119 in β cells induces glucose-dependent insulin secretion via increased intracellular cyclic adenosine monophosphate (8, 13). Several phase II studies of GPR119 agonists, including GSK1292263 (23), MBX-2982 (24), PSN821 (25), LEZ763 (26), and JNJ-38431055 (11, 27), have been conducted, but some evidence of tachyphylaxis was observed, and the results are inconsistent (11, 23, 24). However, in a Phase II study, DS-8500a elicited significant, progressive reductions in blood glucose concentrations 14 to 28 days after the start of administration, and the glucose-lowering effects did not appear to wane or deteriorate with time (14). In our study, DS-8500a demonstrated a significant blood-glucose-lowering effect, and higher total plasma GLP-1 levels were observed in mice treated with DS-8500a (DR+DS) than in those untreated (DR+C), even at the end of the study. Thus, this agent might be suitable for analyzing the long-term efficacy of GPR119 stimulation on BCM *in vivo*.

Progressive loss of pancreatic BCM is a characteristic feature of T2DM (1). The major factors contributing to the progressive loss of BCM include gluco- and lipo-toxicity, inflammation, and oxidative stress (28, 29, 30, 31). Even at the time of a diagnosis of diabetes, the pancreatic BCM deficit is estimated to be over 40%–50% (32, 33, 34). Therefore, preserving or increasing the BCM is a critical strategy for the prevention and long-term management of the disease. Despite this urgent need, accurate quantification of BCM *in vivo* and in humans has been challenging. However, major progress has been made recently in the development of both tracers and detection methods (2). In the search for ideal tracers with reasonably high affinities and sensitivities for the specific structure of β cells, GLP-1 receptor agonists (3, 35) as well as antagonists (36, 37) have been proposed. In particular, the use of GLP-1 agonists as radiotracers is highly promising for *in vivo* β-cell imaging by PET or SPECT (35, 38). [Lys12(^{111}In-BnDTPA-Ahx)]exendin-4 yields a reasonable correlation in intensity between BCM and SPECT (3, 5, 39). The present study demonstrates that ^{111}In-exendin-4 SPECT/CT clearly revealed the difference in BCM between the three groups of db/db mice (Figure 4B). Therefore, our ^{111}In-exendin-4 SPECT/CT technique might be useful for the *in vivo* comparison of BCM in the evaluation of the efficacy of diabetes therapies.

The chronic effects of GPR119 agonists on BCM have not been fully examined. Panaro BL et al. reported that β-cell specific inactivation of GPR119 didn't affect glucose-stimulated insulin secretion (40). On the other hand, Ansarullah et al. reported that the

GPR119 agonist PSN632408 stimulated β-cell replication, improved islet graft functions, and increased the pancreatic BCM in mice with STZ-induced diabetes (9, 10), suggesting that β-cell replication is mediated through GPR119 (9). Furthermore, as GPR119 agonists stimulate GLP-1 secretion from intestinal L cells, they could induce β-cell replication and neogenesis in addition to protecting against cellular apoptosis through GLP-1 action (41, 42). In our study, the β-cell replication ratio in mice treated with DS-8500a under dietary restriction was significantly higher than that of mice treated with dietary restriction alone (Figure 5C). On the other hand, the β-cell apoptosis ratio in mice treated with DS-8500a under dietary restriction tended to be lower than that of mice treated with dietary restriction alone although no significant difference between the two groups (Figure 5D). Therefore, BCM preservation by DS-8500a might be explained in part by the stimulation of β-cell proliferation, as in the previous study of PSN632408 (9, 10). Unfortunately, it remains unclear to what extent GPR119 on pancreatic β cells and GLP-1 contribute to the observed BCM preservation by GPR119 agonists. Further studies of mice with GLP-1 receptor knockout or β-cell-specific GPR119 knockout are warranted to address this issue.

We demonstrated the longitudinal changes in *in vivo* pancreatic RI intensities of all groups of mice using ^{111}In-exendin-4 SPECT/CT (Figure 4A). The trends in BCM changes suggested here are consistent with those of previous report (43), although no longitudinal data have been reported previously. Moreover, the difference in pancreatic RI intensity between the DR+C and DR+DS mice seems to be reasonable in light of the results of glucose intolerance during the observation (Figure 2A and 2B) and histological findings at 13 weeks of age (Figure 5A). These results suggest that the longitudinal changes in pancreatic RI intensity shown by ^{111}In-exendin-4 SPECT/CT analysis reasonably reflect the real-time BCM changes.

Finally, we also note that the relatively small number of mice for the imaging analysis in this study might prevent more robust conclusions about how well ^{111}In-exendin-4 SPECT/CT can follow BCM changes. In addition, a possible increase in GLP-1 receptor expression followed by GPR119 agonism might be considered as another possibility for the apparent increase of pancreatic uptake values on ^{111}In-exendin-4 SPECT/CT in DR+DS mice. Although the relationship between the expression level of GLP-1 receptor and GPR119 stimulation has not been examined, pancreatic uptake values on ^{111}In-exendin-4 SPECT/CT in this study are not likely to be affected since all groups of mice showed the linear correlation between pancreatic uptake values on ^{111}In-exendin-4 SPECT/CT and histological BCM (Figure 5B). Moreover, transcriptomic analyses of purified α cells showed high expression levels of GPR119 (44, 45); an increase in cells double positive for insulin and

glucagon could plausibly increase pancreatic uptake values on ^{111}In-exendin-4 SPECT/CT. However, the robust changes of double positive cells for insulin and glucagon in mice with GPR119 agonist treatment and/or GPR119 knock out mice have not been clarified (9, 32). In addition, pancreatic uptake values on ^{111}In-exendin SPECT/CT were not affected by α-cell mass itself (46). The further accumulation of BCM data with longitudinal observations *in vivo* is needed.

In conclusion, the GPR119 agonist DS-8500a attenuated the progression of BCM loss in prediabetic db/db mice beyond that of dietary restriction alone. This result was also demonstrated using ^{111}In-exendin-4 SPECT/CT *in vivo*.

Funding

This study was supported by grants from Daiichi Sankyo Company, Ltd.

Daiichi-Sankyo http://dx.doi.org/10.13039/501100002973, Nobuya Inagaki

Contribution statement

T.M. planned the study, analyzed data, contributed to discussions, and wrote, reviewed, and edited the manuscript. H.F. planned the study, contributed to discussions, and reviewed the manuscript. N.F. and K.H. contributed to data analysis and discussions. K.M. planned the study, analyzed data, and contributed to discussions. N.I. contributed to discussions and reviewed and edited the manuscript. All authors reviewed the results and approved the final version of the manuscript.

Corresponding author: Nobuya Inagaki M.D., Ph D, 54 Kawahara-cho, Shogoin, Sakyo-ku, Kyoto 606-8507, Japan, TEL: +81-75-751-3562, FAX: +81-75-751-6601, Email: inagaki@kuhp.kyoto-u.ac.jp

Disclosure statement:

N.I. received clinical commissioned/joint research grants from Daiichi Sankyo Company, Ltd. for this research. N.I. also received research funds from Mitsubishi Tanabe Pharma Co., Daiichi Sankyo Co., Ltd., and AstraZeneca; received speaker honoraria from Kowa Pharmaceutical Co., Ltd.; received scholarship grant from Kissei Pharmaceutical, Taisho Toyama Pharmaceutical, Sanofi, Mitsubishi Tanabe Pharma, Takeda, Japan Tobbaco, Kyowa Kirin, Sumitomo Dainippon Pharma, Astellas Pharma, MSD, Eli Lilly Japan, Ono Pharmaceutical, Sanwa Kagaku Kenkyusho, Nippon Boehringer Ingelheim, Novo Nordisk Pharma, Novartis Pharma, and Teijin Pharma. T.M., H.F., N.F., K.H., and K.M. have no conflict of interest to disclose.

Data Availability

All data generated or analyzed during this study are included in this published article or in the data repositories listed in References.

References

1, Rhodes C.J. Type 2 diabetes-a matter of beta-cell life and death? *Science*. 2005;307(5708):380-384.

2, Tiedge M. Inside the pancreas: progress and challenges of human beta cell mass quantification. *Diabetologia*. 2014;57(5):856-859.

3, Kimura H, Fujita N, Kanbe K, Matsuda H, Watanabe H, Arimitsu K, Fujimoto H, Hamamatsu K, Yagi Y, Ono M, Inagaki N, Saji H. Synthesis and biological evaluation of an ^{111}In-labeled exendin-4 derivative as a single-photon emission computed tomography probe for imaging pancreatic β-cells. *Bioorg Med Chem.* 2017;25(20):5772-5778.

4, Hamamatsu K, Fujimoto H, Fujita N, Murakami T, Kimura H, Saji H, Inagaki N. Establishment of a method for in-vivo SPECT/CT imaging analysis of 111In-labeled exendin-4 pancreatic uptake in mice without the need for nephrectomy or a secondary probe. *Nucl Med Biol.* 2018;64-65:22-27.

5, Fujita N, Fujimoto H, Hamamatsu K, Murakami T, Kimura H, Toyoda K, Saji H, Inagaki N. Non-invasive longitudinal quantification of beta cell mass with ^{111}Indium-labeled exendin-4. *FASEB J.* 2019 doi: 10.1096/fj.201900555RR.

6, Chu ZL, Carroll C, Alfonso J, Gutierrez V, He H, Lucman A, Pedraza M, Mondala H, Gao H, Bagnol D, Chen R, Jones RM, Behan DP, Leonard J. A role for intestinal endocrine cell-expressed g protein-coupled receptor 119 in glycemic control by enhancing glucagon-like peptide-1 and glucose-dependent insulinotropic peptide release. *Endocrinology.* 2008;149(5):2038-2047.

7, Odori S, Hosoda K, Tomita T, Fujikura J, Kusakabe T, Kawaguchi Y, Doi R, Takaori K, Ebihara K, Sakai Y, Uemoto S, Nakao K. GPR119 expression in normal human tissues and islet cell tumors: evidence for its islet-gastrointestinal distribution, expression in pancreatic beta and alpha cells, and involvement in islet function. *Metabolism.* 2013;62(1):70-78.

8, Chu ZL, Jones RM, He H, Carroll C, Gutierrez V, Lucman A, Moloney M, Gao H, Mondala H, Bagnol D, Unett D, Liang Y, Demarest K, Semple G, Behan DP, Leonard J. A role for beta-cell-expressed G protein-coupled receptor 119 in glycemic control by enhancing glucose-dependent insulin release. *Endocrinology.* 2007;148(6):2601-2609.

9, Ansarullah, Lu Y, Holstein M, DeRuyter B, Rabinovitch A, Guo Z. Stimulating β-cell regeneration by combining a GPR119 agonist with a DPP-IV inhibitor. *PLoS One*. 2013;8(1):e53345.

10, Gao J, Tian L, Weng G, Bhagroo NV, Sorenson RL, O'Brien TD, Luo J, Guo Z. Stimulating beta cell replication and improving islet graft function by GPR119 agonists. *Transpl Int.* 2011;24(11):1124-1134.

11, Katz LB, Gambale JJ, Rothenberg PL, Vanapalli SR, Vaccaro N, Xi L, Sarich TC, Stein PP. Effects of JNJ-38431055, a novel GPR119 receptor agonist, in randomized, double-blind, placebo-controlled studies in subjects with type 2 diabetes. *Diabetes Obes Metab.* 2012;14(8):709-716.

12, Nunez DJ, Bush MA, Collins DA, McMullen SL, Gillmor D, Apseloff G, Atiee G, Corsino L, Morrow L, Feldman PL. Gut hormone pharmacology of a novel GPR119 agonist (GSK1292263), metformin, and sitagliptin in type 2 diabetes mellitus: results from two randomized studies. *PLoS One.* 2014;9(4):e92494.

13, Matsumoto K, Yoshitomi T, Ishimoto Y, Tanaka N, Takahashi K, Watanabe A, Chiba K. DS-8500a, an orally available G protein-coupled receptor 119 agonist, upregulates glucagon-like peptide-1 and enhances glucose-dependent insulin secretion and improves glucose homeostasis in type 2 diabetic rats. *J Pharmacol Exp Ther.* 2018;367(3):509-517.

14, Inagaki N, Chou HS, Tsukiyama S, Washio T, Shiosakai K, Nakatsuka Y, Taguchi T. Glucose-lowering effects and safety of DS-8500a, a G protein-coupled receptor 119 agonist, in Japanese patients with type 2 diabetes: results of a randomized, double-blind, placebo-controlled, parallel-group, multicenter, phase II study. *BMJ Open Diabetes Res Care.* 2017;5(1):e000424.

15, RRID: AB_2801383 , https://antibodyregistry.org/search.php?q=AB_2801383

16, RRID: AB_2811268 , https://antibodyregistry.org/search.php?q=AB_2811268

17, RRID: AB_2126540 , https://antibodyregistry.org/search?q=AB_2126540

18, RRID: AB_143165 , https://antibodyregistry.org/search?q=AB_143165

19, RRID: AB_306130 , https://antibodyregistry.org/search?q=AB_306130

20, RRID: AB_443209 , https://antibodyregistry.org/search?q=AB_443209

21, RRID: AB_2736871 , https://antibodyregistry.org/search.php?q=AB_2736871

22, RRID: AB_2534093 , https://antibodyregistry.org/search?q=AB_2534093

23, Nunez DJ, Bush MA, Collins DA, McMullen SL, Gillmor D, Apseloff G, Atiee G, Corsino L, Morrow L, Feldman PL. Gut hormone pharmacology of a novel GPR119 agonist (GSK1292263), metformin, and sitagliptin in type 2 diabetes mellitus: results from two randomized studies. *PLoS One.* 2014;9(4):e92494.

24, Roberts B, Gregoire FM, Karpf DB, Clemens E, Lavan B, Johnson J, Mcwherter CA, Martin R, Wilson M. MBX-2982, a novel oral GPR119 agonist for the treatment of type 2 diabetes: results of single & multiple dose studies. *Diabetes.* 2009;58(Suppl 1):Abstract 164-OR.

25, Goodman ML, Dow J, Van Vliet AA, Pleszko A, Lockton JA. Orally administered GPR119 agonist PSN821 shows clinically significant glucose lowering and other potential cardiometabolic benefits in patients with T2DM. *Diabetologia.* 2011;54:Abstract OP32.

26, He Y, Davis L, Bhad P, Amer A, Colin L, Yan JH, Harris S, Taylor A. LEZ763, a novel GPR119 agonist, increases GLP-1, GIP, PYY, and glucagon, but has minimal effects on glucose in patients with type 2 diabetes. *Diabetes.* 2015;64(Suppl 1):122–LB.

27, Katz LB, Gambale JJ, Rothenberg PL, Vanapalli SR, Vaccaro N, Xi L, Polidori DC, Vets E, Sarich TC, Stein PP. Pharmacokinetics, pharmacodynamics, safety, and tolerability of JNJ-38431055, a novel GPR119 receptor agonist and potential antidiabetes agent, in healthy male subjects. *Clin Pharmacol Ther.* 2011;90(5):685–692.

28, Maedler K, Sergeev P, Ris F, Oberholzer J, Joller-Jemelka HI, Spinas GA, Kaiser N, Halban PA, Donath MY. Glucose-induced beta cell production of IL-1beta contributes to glucotoxicity in human pancreatic islets. *J Clin Invest.* 2002;110(6):851-860.

29, Maedler K, Sergeev P, Ehses JA, Mathe Z, Bosco D, Berney T, Dayer JM, Reinecke M, Halban PA, Donath MY. Leptin modulates beta cell expression of IL-1 receptor antagonist and release of IL-1beta in human islets. *Proc Natl Acad Sci U S A.* 2004;101(21):8138-8143.

30, Cnop M, Welsh N, Jonas JC, Jörns A, Lenzen S, Eizirik DL. Mechanisms of pancreatic beta-cell death in type 1 and type 2 diabetes: many differences, few similarities. *Diabetes.* 2005;54(Suppl 2):S97-107.

31, Robertson RP. Chronic oxidative stress as a central mechanism for glucose toxicity in pancreatic islet beta cells in diabetes. *J Biol Chem.* 2004;279(41):42351-42354.

32, U.K. Prospective Diabetes Study Group. U.K. prospective diabetes study 16. Overview of 6 years' therapy of type II diabetes: a progressive disease. U.K. *Diabetes.* 1995;44(11):1249-1258.

33, Butler AE, Janson J, Bonner-Weir S, Ritzel R, Rizza RA, Butler PC. Beta-cell deficit and increased beta-cell apoptosis in humans with type 2 diabetes. *Diabetes.* 2003;52(1):102–110.

34, Kloppel G, Lohr M, Habich K, Oberholzer M, Heitz PU. Islet pathology and the pathogenesis of type 1 and type 2 diabetes mellitus revisited. *Surv Synth Pathol Res.* 1985;4(2):110–125.

35, Gotthardt M, Lalyko G, van Eerd-Vismale J, Keil B, Schurrat T, Hower M, Laverman P, Behr TM, Boerman OC, Göke B, Béhé M. A new technique for in vivo imaging of specific GLP-1 binding sites: first results in small rodents. *Regul Pept.* 2006;137(3):162–167.
36, Mukai E, Toyoda K, Kimura H, Kawashima H, Fujimoto H, Ueda M, Temma T, Hirao K, Nagakawa K, Saji H, Inagaki N. GLP-1 receptor antagonist as a potential probe for pancreatic beta-cell imaging. *Biochem Biophys Res Commun.* 2009;389(3):523-526.
37, Kimura H, Matsuda H, Ogawa Y, Fujimoto H, Toyoda K, Fujita N, Arimitsu K, Hamamatsu K, Yagi Y, Ono M, Inagaki N, Saji H. Development of 111In-labeled exendin(9-39) derivatives for single-photon emission computed tomography imaging of insulinoma. *Bioorg Med Chem.* 2017;25(4):1406-1412.
38, Brom M, Andralojc K, Oyen WJ, Boerman OC, Gotthardt M. Development of radiotracers for the determination of the beta-cell mass in vivo. *Curr Pharm Des.* 2010;16(14):1561–1567.
39, Brom M, Woliner-van der Weg W, Joosten L, Frielink C, Bouckenooghe T, Rijken P, Andralojc K, Göke BJ, de Jong M, Eizirik DL, Béhé M, Lahoutte T, Oyen WJ, Tack CJ, Janssen M, Boerman OC, Gotthardt M. Non-invasive quantification of the beta cell mass by SPECT with ^{111}In-labelled exendin. *Diabetologia.* 2014;57(5):950-959.
40, Panaro BL, Flock GB, Campbell JE, Beaudry JL, Cao X, Drucker DJ. β-Cell inactivation of *Gpr119* unmasks incretin dependence of GPR119-mediated glucoregulation. *Diabetes.* 2017;66(6):1626-1635.
41, Xu G, Stoffers DA, Habener JF, Bonner-Weir S. Exendin-4 stimulates both beta-cell replication and neogenesis, resulting in increased beta-cell mass and improved glucose tolerance in diabetic rats. *Diabetes.* 1999;48(12):2270-2276.
42, Li Y, Hansotia T, Yusta B, Ris F, Halban PA, Drucker DJ. Glucagon-like peptide-1 receptor signaling modulates beta cell apoptosis. *J Biol Chem.* 2003;278(1):471-478.
43, Puff R, Dames P, Weise M, Göke B, Seissler J, Parhofer KG, Lechner A. Reduced proliferation and a high apoptotic frequency of pancreatic beta cells contribute to genetically-determined diabetes susceptibility of db/db BKS mice. *Horm Metab Res.* 2011;43(5):306-311.
44, Adriaenssens AE, Svendsen B, Lam BY, Yeo GS, Holst JJ, Reimann F, Gribble FM. Transcriptomic profiling of pancreatic alpha, beta and delta cell populations identifies delta cells as a principal target for ghrelin in mouse islets. Diabetologia. 2016;59(10):2156-2165.
45, Segerstolpe Å, Palasantza A, Eliasson P, Andersson EM, Andréasson AC, Sun X, Picelli S, Sabirsh A, Clausen M, Bjursell MK, Smith DM, Kasper M, Ämmälä C, Sandberg R.

Single-Cell Transcriptome Profiling of Human Pancreatic Islets in Health and Type 2 Diabetes. *Cell Metab*. 2016;24(4):593-607.

46, Brom M, Joosten L, Frielink C, Boerman O, Gotthardt M. (111)In-exendin uptake in the pancreas correlates with the β-cell mass and not with the α-cell mass. *Diabetes.* 2015;64(4):1324-1328.

Figure 1. Dietary consumption, bodyweight, non-fasting blood glucose, and mouse glycohemoglobin levels during observation. Weekly dietary consumption (A), bodyweight (B), non-fasting blood glucose (C), and db/db mouse glycohemoglobin (D) levels during the observation period. Db/db mice were treated as follows: without dietary restriction (DR-C), green triangles and bars (n = 4); with dietary restriction alone (DR+C), blue rhombi and bars (n = 7); with DS-8500a and dietary restriction (DR+DS), red squares and bars (n = 8). The data are expressed as the mean ± SD. DR-C vs. DR+C, $^{\#}P < 0.05$, $^{\#\#}P < 0.01$; DR+C vs. DR+DS, $^{*}P < 0.05$; DR-C vs. DR+DS, $^{\dagger}P < 0.05$, $^{\dagger\dagger}P < 0.01$; N.S., not significant.

Figure 2. Blood glucose and insulin levels during OGTT. Blood glucose and insulin levels (A), and AUC-glucose and -insulin (B) during OGTT at 5 (baseline), 9, and 13 weeks of age. DR-C, green triangles and bars (n = 4); DR+C, blue rhombi and bars (n = 7); DR+DS, red squares and bars (n = 8). The data are expressed as the mean ± SD. DR-C vs. DR+C, $^{\#\#}P < 0.01$; DR+C vs. DR+DS, $^{*}P < 0.05$; DR-C vs. DR+DS; $^{\dagger}P < 0.05$; N.S., not significant.

Figure 3. Representative images of *in vivo* ^{111}In-exendin-4 SPECT/CT. Representative ^{111}In-exendin-4 SPECT/CT images of 13-week-old db/db mice. Coronal and axial images are shown in upper and lower panels, respectively. Maximum to minimum intensity: red > orange > yellow > green > blue > black. Signals from the pancreas, blue arrows and circles; Signals from the kidney, yellow brown arrows and circles. L, left; R, right; V, ventral.

Figure 4. *In vivo* SPECT/CT and *ex vivo* pancreas analysis using ^{111}In-exendin-4 probe. Longitudinal changes in the pancreatic uptake values (%ID/g) demonstrated by *in vivo* ^{111}In-exendin-4 SPECT/CT in DR+C and DR+DS mice during the 8-week observation period (A). Cross-sectional analysis of the pancreatic uptake values (B) and *ex vivo* RI counts of pancreas per injected dose of the probe (%ID/g tissue) (C) in 13-week-old db/db mice under three different interventions: DR-C, green triangles and bars (n = 3); DR+C, blue rhombi and bars (n = 3); DR+DS, red squares and bars (n = 3). The data are expressed as the mean ± SD. DR-C vs. DR+C, $^{\#}P < 0.05$, $^{\#\#}P < 0.01$; DR+C vs. DR+DS, $^{*}P < 0.05$, $^{**}P < 0.01$; DR-C vs. DR+DS, $^{\dagger\dagger}P < 0.01$.

Figure 5. Histological quantification of BCM and immunohistochemical analysis of proliferation and apoptosis of β cells in db/db mice. (A) BCM calculated by histological analysis in DR-C (n = 3), DR+C (n = 3), and DR+DS (n = 3) mice (left column). Representative images of insulin-positive area of pancreas in each group (right column). (B) Significant correlation between pancreatic uptake values on ^{111}In-exendin-4 SPECT/CT (%ID/g) and BCM calculated by histological analysis in 13-week-old db/db mice (n=9). (C) Ratio of insulin/Ki67/DAPI co-positive cells to total insulin-positive cells in 13-week-old mice of DR+C (n = 7) and DR+DS (n = 8) groups. (D) Ratio of insulin/TUNEL/DAPI co-positive cells to total insulin-positive cells in 13-week-old mice of DR+C (n = 7) and DR+DS (n = 8) groups. DR-C, DR+C, and DR+DS mice are represented by green, blue, and red bars, respectively. The data are expressed as the mean ± SD. Scale bar indicates 300 μm. DR+C vs. DR+DS, $^{*}P < 0.05$; DR-C vs. DR+DS, $^{\dagger\dagger}P < 0.01$; N.S., not significant.

Figure 1.

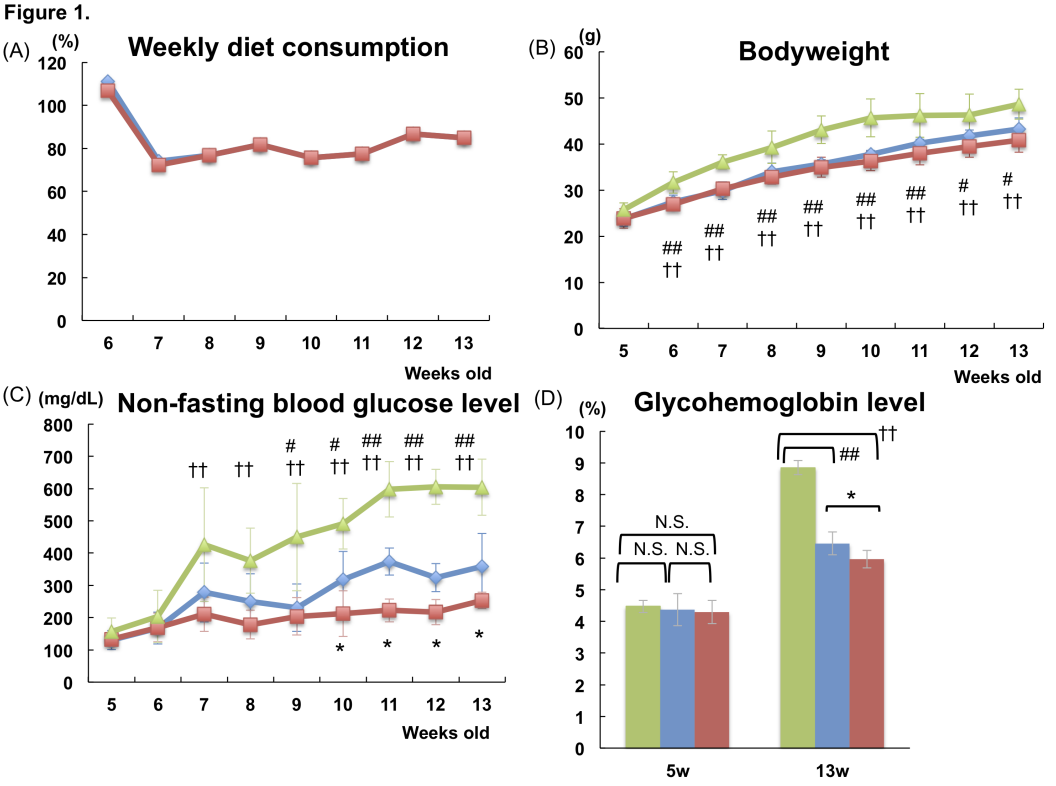

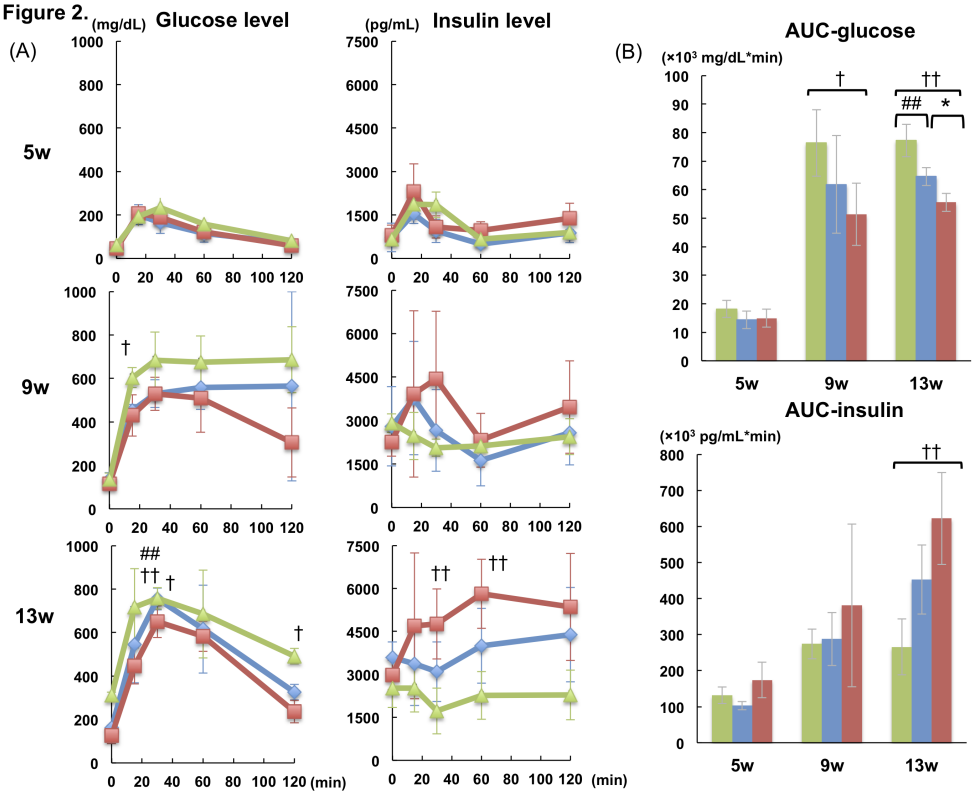

Figure 3.

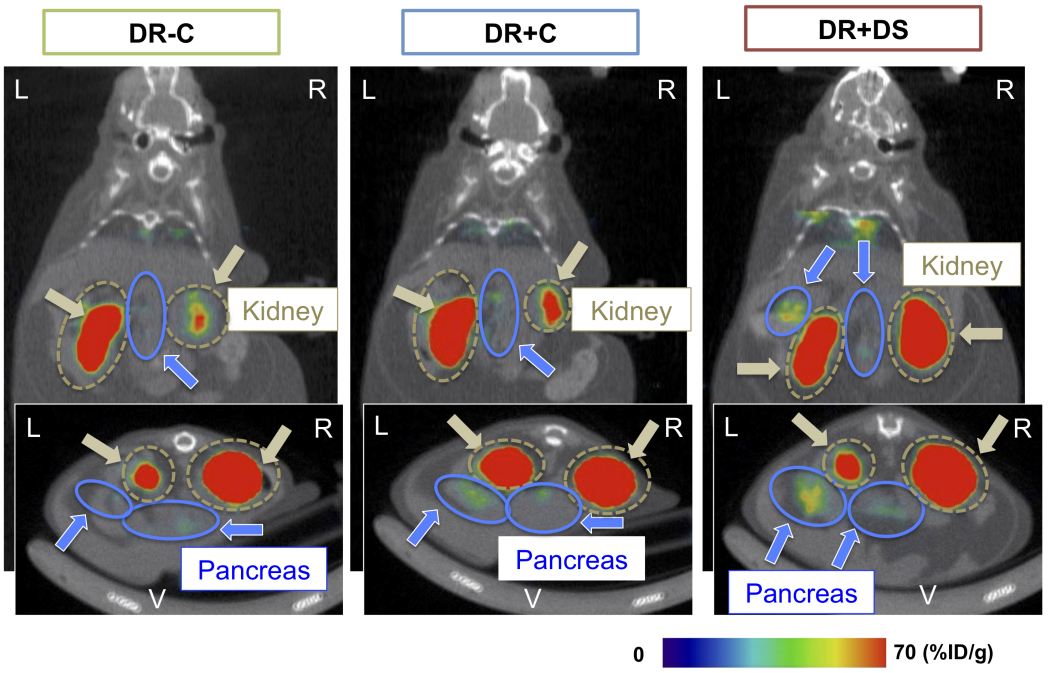

Figure 4.

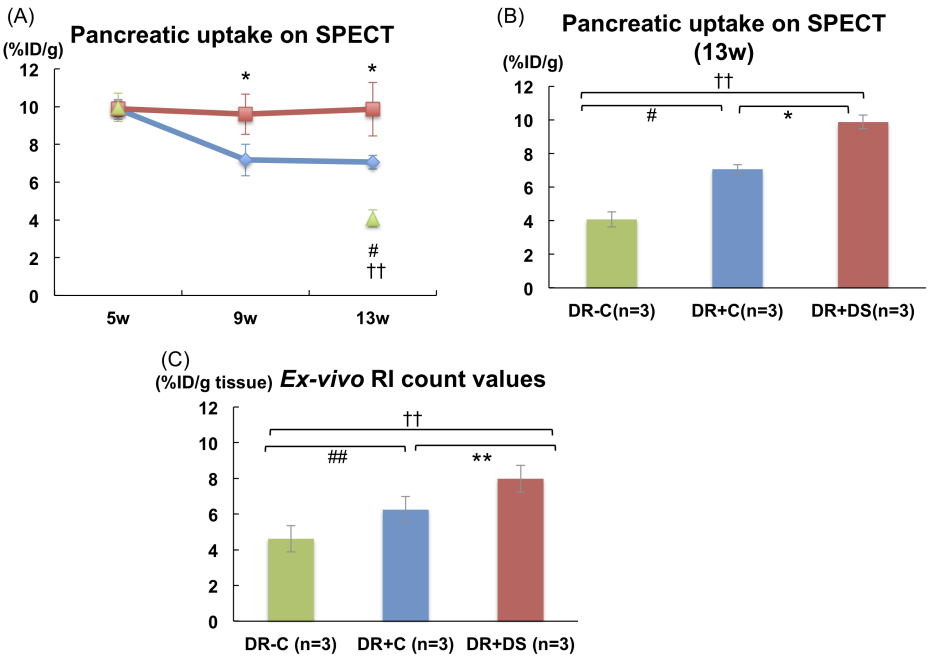

Figure 5.